SCIENTIFIC REP**O**RTS

OPEN

A Three-dimensional Floating Air Cathode with Dual Oxygen Supplies for Energy-efficient Production of Hydrogen Peroxide

Haichuan Zhang[1,2], Yingjie Li[3], Hao Zhang[1,2], Guanghe Li[1,2] & Fang Zhang[1,2]

The *in situ* and cleaner electrochemical production of hydrogen peroxide (H_2O_2) through two-electron oxygen reduction reaction has drawn increasing attentions in environmental applications as an alternative to traditional anthraquinone process. Air cathodes avoid the need of aeration, but face the challenges of declined performance during scale-up due to non-uniform water infiltration or even water leakage, which is resulted from changing water pressures and immature cathode fabrication at a large scale. To address these challenges, a three-dimensional (3-D) floating air cathode (FAC) was built around the commercial sponge, by coating with carbon black/poly(tetrafluoroethylene) using a simple dipping-drying method. The FAC floated on the water-air interface without extensive water-proof measures, and could utilize oxygen both from passive diffusion and anodic oxygen evolution to produce H_2O_2. The FAC with six times of dipping treatment produced a maximum H_2O_2 concentration of $177.9 \pm 26.1\,mg\,L^{-1}$ at 90 min, with low energy consumption of $7.1 \pm 0.003\,Wh\,g^{-1}$ and stable performance during 10 cycles of operation. Our results showed that this 3-D FAC is a promising approach for *in situ* H_2O_2 production for both environmental remediation and industrial applications.

Hydrogen peroxide (H_2O_2), as a green, powerful and versatile oxidant, has been widely applied either alone or as a reagent of advanced oxidation processes (e.g., Fenton/Fenton-like reactions[1,2], $TiO_2/H_2O_2/UV$ photocatalysis[3,4], ozone treatment[2]) for water/wastewater treatment, disinfectant and paper-blenching applications[2,5,6]. At present, H_2O_2 is commercially produced using the anthraquinone process in large-scale facilities, involving the sequential hydrogenation and oxidation of anthraquinone molecules[7,8]. This process is inherently complex and energy-intensive (1–2 dollars per kilogram), in which anthraquinone and its derivative are carcinogenic compounds[9]. Although H_2O_2 is not considered an explosive, the transportation, storage and handling of concentrated solutions need special safety precautions[10,11]. Therefore, many researchers now focus on the *in situ*, continuous and cleaner production of H_2O_2, primarily via the two-electron oxygen reduction reaction (ORR, $O_2 + 2H^+ + 2e^- \rightarrow H_2O_2$)[12,13].

Due to the limit of low solubility (8.1–8.5 ppm at 25 °C)[14,15] and small diffusion coefficient ($D_{O_2,water}$ of 1.96–$2.56 \times 10^{-9}\,m^2\,s^{-1}$ at 25 °C)[16,17] of oxygen in water, oxygen mass transfer has been recognized as an important rate-limiting step of oxygen reduction reaction (ORR)[18,19]. The air cathode, in which a hydrophobic gas diffusion layer (GDL) directly exposes to air ($D_{O_2,\,GDL}$ of $3.0 \times 10^{-6}\,m^2\,s^{-1}$) and thus oxygen passively diffuses to its catalyst layer (CL, $D_{O_2,\,CL}$ $3.0 \times 10^{-7}\,m^2\,s^{-1}$)[20], no longer depends on the feed of dissolved oxygen in the electrolyte solution. The binders of GDL and CL are often superhydrophobic polymers, such as poly(dimethylsiloxane)[21] and poly(tetrafluoroethylene) (PTFE)[22], maintaining the O_2 diffusion path and preventing catalyst flooding. Many reactors based on air cathode, such as stacked electrosynthesis reactor[23] and divided-cell trickle bed electrochemical reactor[24], were designed and applied for H_2O_2 production. When air cathodes are scaled up for practical applications, it is difficult to achieve uniform water infiltration due to both changing water pressures at different

[1]School of Environment and State Key Joint Laboratory of Environment Simulation and Pollution Control, Tsinghua University, Beijing, 100084, China. [2]Key Laboratory for Solid Waste Management and Environment Safety (Tsinghua University), Ministry of Education of China, Tsinghua University, Beijing, 100084, China. [3]Department of Materials Science and Engineering, College of Engineering, Peking University, Beijing, 100871, P. R. China. Correspondence and requests for materials should be addressed to F.Z. (email: fangzhang@tsinghua.edu.cn)
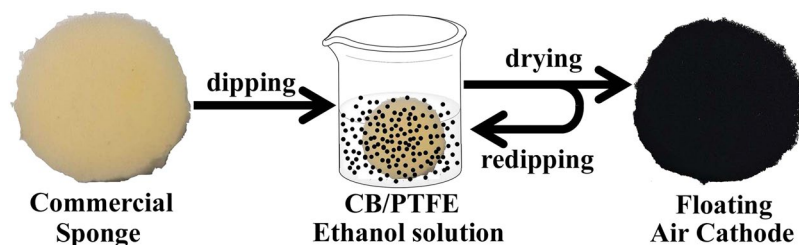
Figure 1. Schematic illustration of floating air cathode via the dipping-drying process.

depth and immature GDL fabrication at a large scale[25,26]. This uneven water infiltration resulted in either water leakage, or a non-uniform current distribution within the cathode, leading to degraded cathode performance[25,26].

The electrochemical ORR systems often rely on single external O_2 supply methods such as passive oxygen diffusion or active aeration, but neglect the produced O_2 from the anodic oxygen evolution reaction (OER)[10,19,27]. In the two-electron oxygen reduction process, the produced O_2 from the OER anode is half of that consumed at the cathode[10,28], but this part of O_2 is often wasted. Recently, with the utilization of anodically produced oxygen, we developed an oxygen-self-supplied electro-fenton system with dual cathodes that did not need the feed of external O_2 supply[10]. Similar approaches that utilize the anodically produced oxygen extend the application field of *in situ* electrochemical H_2O_2 production[3,29]. In spite of much work on single oxygen supply[18,30], the electrochemical system to produce H_2O_2 with multi-oxygen supplies is rarely reported. In addition, it is really significant to figure out contributions of different O_2 supplies to H_2O_2 production for the future practical applications.

In this study, in order to address the uneven water infiltration issues and enhance the O_2 mass transfer to air cathodes for scale up applications, we developed a floating air cathode (FAC) using the commercially available poly(urethane) (PU) sponge that floats at the solution/air interface for effective H_2O_2 production without the needs of extensive water-proof measures. The sponge was dipped in the catalyst ink made of carbon black to make it electrically conductive and electrochemically active. The FAC with various dipping times (DTs) was characterized in terms of morphology, mass loading, ohmic resistance (R_{ohm}), and electrochemically active surface area (ECSA). The FAC performance in terms of H_2O_2 concentration and normalized energy consumption were also evaluated to find the most cost-effective catalyst loading for the production of H_2O_2. We examined the H_2O_2 production with different relative positions of the cathode in the electrolyte, to characterize the influence of O_2 supply sources (passive diffusion from air, and O_2 produced from the OER anode) to the ORR system.

Methods

Electrode Preparation. The floating air cathode (FAC) was fabricated through a simple and scalable dipping and drying process (Fig. 1)[31], around the commercially available PU sponge of 50 pores per inch (ppi) as the support (Hangmei sponge Co., Ltd). Carbon black (CB, acetylene, 50% compressed, Alfra Aesar Co., Ltd) was used both as the catalyst and the conductive layer, with PTFE (60 wt.% dispersion in H_2O, Sigma-aldrich Co., Ltd) as the binder. CB (300 mg) and 60% PTFE (2 mL) with PTFE/CB ratio of 6:1 were dispersed in 30 mL of ethanol with ultrasonication of 30 min to form a uniform suspension. The sponge was dipped into the suspension and dried in the electric oven at 80 °C for several times[31]. The FAC had a diameter of 4.0 centimeters (cm, projected surface area of 12.56 cm², 1.0 cm in height), and catalyst loading depended on the dipping times. Mixed metal oxides (MMO) mesh (4.0 cm in diameter × 0.1 cm height) was used as the anode.

Operation. All the electrochemical measurements were performed in Petri dishes (6.0 cm inner diameter × 3.0 cm height or 9.0 cm inner diameter × 2.0 cm height, Fig. S1) with 50 mL electrolyte (100 mM Na_2SO_4 solution). The FAC floated at the solution/air interface, and the MMO anode was placed at the bottom of the reactor and facing the FAC. The electrode spacing between the bottom of FAC and the top of MMO was ~2.0 cm. The electrochemical double-layer capacitance (EDLC) measurements of FACs with different dipping times were carried out using cyclic voltammetry between −0.04 and 0.04 V versus Ag/AgCl with the scan rate of 0.5 mV s⁻¹, which served as an estimate of the electrochemically active surface area (ECSA) of the solid-liquid interface[32,33]. FACs with different dipping times were measured by linear sweep voltammetry (LSV) from 0 to −1.0 V versus Ag/AgCl with the scan rate of 5 mV s⁻¹ to evaluate their ORR performance. The production of H_2O_2 was measured at a fixed voltage of 2 V using the potentiostat (VMP3, BioLogic, France). Cathode potentials were measured by the Keithley data acquisition system (2700 multimeter, Keithley, America) versus the Ag/AgCl reference electrodes (all cathode potentials were reported versus Ag/AgCl). Under the same mode with the fixed voltage of 2 V, the FAC of DT6 was chosen to evaluate the stability of H_2O_2 generation by changing the electrolyte every 90 min for 10 times. The produced H_2O_2 concentrations were measured with different applied voltages using the FAC of DT6.

To investigate the influence of oxygen supply on system performance, four types of working modes were designed (Fig. S1), including: the mode as mentioned above with the floating air cathode facing the OER anode (Mode 1, M1, oxygen from both air and OER), floating air cathode misplaced with OER anode (Mode 2, M2, oxygen only from air), submerged cathode facing the OER anode (Mode 3, M3, oxygen from OER) and submerged cathode misplaced with OER anode (Mode 4, M4, no continuous oxygen supply). The produced H_2O_2 concentrations under different working modes were measured, under the same set voltage of 2 V.

Analysis and Calculations. Scanning electron microscopy (SEM) images of FACs were taken on a JEOL JSM7001 scanning electron microscope with the accelerating voltage of 20 kV. The ohmic resistance was monitored by the digital multimeter (DM-A, Jetech Co. Ltd., China), and mass loading of the catalyst was calculated based on the weight difference measured by electronic balance (ME-104, Mettler Toledo, China).

The concentration of H_2O_2 standard solution was quantified by a classical potassium permanganate titration based on the below reaction ($5H_2O_2 + 2MnO_4^-$(red) $+ 6H^+ \rightarrow 2Mn^{2+}$(colorless) $+ 5O_2 + 8H_2O$). The calculation of H_2O_2 concentration (c, g L^{-1}) was

$$c(H_2O_2) = \frac{c(KMnO_4) \times V(KMnO_4) \times M(H_2O_2) \times 5}{M(KMnO_4) \times V(H_2O_2) \times 2}$$

where $c(KMnO_4)$ was the concentration of $KMnO_4$ standard solution (g L^{-1}), $V(KMnO_4)$ the volume of consumed $KMnO_4$ standard solution (L), $M(KMnO_4)$ the molar mass of $KMnO_4$ (158 g mol^{-1}), $M(H_2O_2)$ the molar mass of H_2O_2 (34 g mol^{-1}) and $V(H_2O_2)$ the volume of titrated H_2O_2 standard solution (L).

The H_2O_2 concentration of sample was measured by titanium potassium oxalate method[10,19] with a UV-vis spectrophotometer (UV-6850, Jenway, Britain). In the titanium potassium oxalate method, 200 mg L^{-1} of H_2O_2 standard solution was prepared by the as-titrated H_2O_2 solution. To obtain the calibration curve, 200 mg L^{-1} H_2O_2 standard solutions of 0.1 mL, 0.2 mL, 0.3 mL, 0.4 mL and 0.5 mL were added into 0.5 mL $K_2TiO(C_2O_4)_2$ (25 mmol L^{-1}) in H_2SO_4 (1 mol L^{-1}) solution, and then diluted with deionized water to 1 mL, and finally measured by a UV-vis spectrophotometer at the wavelength of 400 nm. Based on the linear relationship between the signal intensity and H_2O_2 concentration, the H_2O_2 concentrations of samples could be obtained. 0.5 mL of solution in each sample was collected for the quantification of H_2O_2 and then 0.5 mL of initial blank solution was added into the electrochemical system to maintain the volume of electrolyte.

The calculation of energy consumption (EC, Wh g^{-1})[22] was

$$EC = \frac{E \times \int I\, dt}{3600 \times c(H_2O_2) \times V}$$

where I was the ORR current (A), E the fixed voltage of 2 V, t the operation time (s), V the volume of electrolyte (L) and $c(H_2O_2)$ the concentration of produced H_2O_2 (g L^{-1}).

The calculation of coulombic efficiency (CE, %)[34] was

$$CE = \frac{n \times F \times c(H_2O_2) \times V}{M(H_2O_2) \times \int I\, dt} \times 100\%$$

where I was the ORR current (A), n the number of transferred electrons ($n = 2$), F the Faraday's constant ($F = 96485$ C mol^{-1}), t the operation time (s), V the volume of electrolyte (L), $M(H_2O_2)$ the molar mass of H_2O_2 (34 g mol^{-1}) and $c(H_2O_2)$ the concentration of produced H_2O_2 (g L^{-1}).

Results and Discussion

Characterization of the Floating Air Cathode. The three-dimensional PU sponge that has been commonly used for household cleaning, packaging, filtrating and many other applications, was utilized for the fabrication of the air cathode. The sponge was dipped into a CB/PTFE ethanol solution, allowing the solution to fill the voids and coat the skeletons. The as-formed electrode could freely float on the air/water interface while pumping water in or out the Petri dish, successfully maintaining the O_2 diffusion path from air. Densities of the PU sponge before and after the dipping-drying treatment (0.02 g cm^{-3} for sponge, 0.05–0.12 g cm^{-3} for FAC, Table S1) were far less than that of water, guaranteeing the floating property of sponge-based electrodes.

The small size of CB powder and strong adhesion of PTFE binder enabled the formation of a carbon "skin" that coated on the sponge surface, as compared with SEM images of the sponge before and after the dipping-drying treatment (Fig. 2 and S2). With the increase of dipping times, the CB/PTFE layer became thicker and gradually filled macropores of the sponge (Figs 2 and S2). This CB/PTFE coating changed the color of sponge from yellow to black (Fig. 1) and electrical conductivity of the entire matrix from insulative to conductive (Fig. S3). In the FAC, the mass loading of catalyst and ohmic resistance greatly relied on dipping times. With the increase of DTs from one to four, the mass loading of catalyst hugely increased from 25.2 to 92.1 mg cm^{-2} while ohmic resistance rapidly decreased from 310 Ω to 36 Ω (Fig. 3a). After four times of dipping into the CB/PTFE solution, the mass loading of catalyst and ohmic resistance of FACs tended to be stable. With six times of dipping-drying treatment, the ohmic resistance of PU sponge coated with CB/PTFE mixture was ~31 Ω (Figs 3a and S3b), enabling its function as an electrode in small scale applications.

Effect of dipping times on FAC electrochemical performance. To estimate the electrochemically active surface area (ECSA) of FACs with different dipping times, the electrochemical double-layer capacitance (EDLC) were measured by cyclic voltammetry[35,36]. It showed that the capacitance greatly relied on dipping times of the electrode. With the increasing DTs from one to six, the EDLC of FACs gradually increased from 12.9 to 58.0 mF (Figs 3b and S4), suggesting that the ECSA improved due to the increased catalyst mass loading. Although the measured resistance did not appreciably decrease after four times, the ECSA still improved with a higher catalyst loading. After six times of dipping treatment, the EDLCs of FACs started to be stable (55.7 mF of DT7 and 57.1 mF of DT8, Figs 3b and S4), attributing to their similar mass loading and ohmic resistance to DT6 (97.9 mg cm^{-2} and 32 Ω for DT7, 100.5 mg cm^{-2} and 30 Ω for DT8, Fig. 3a).
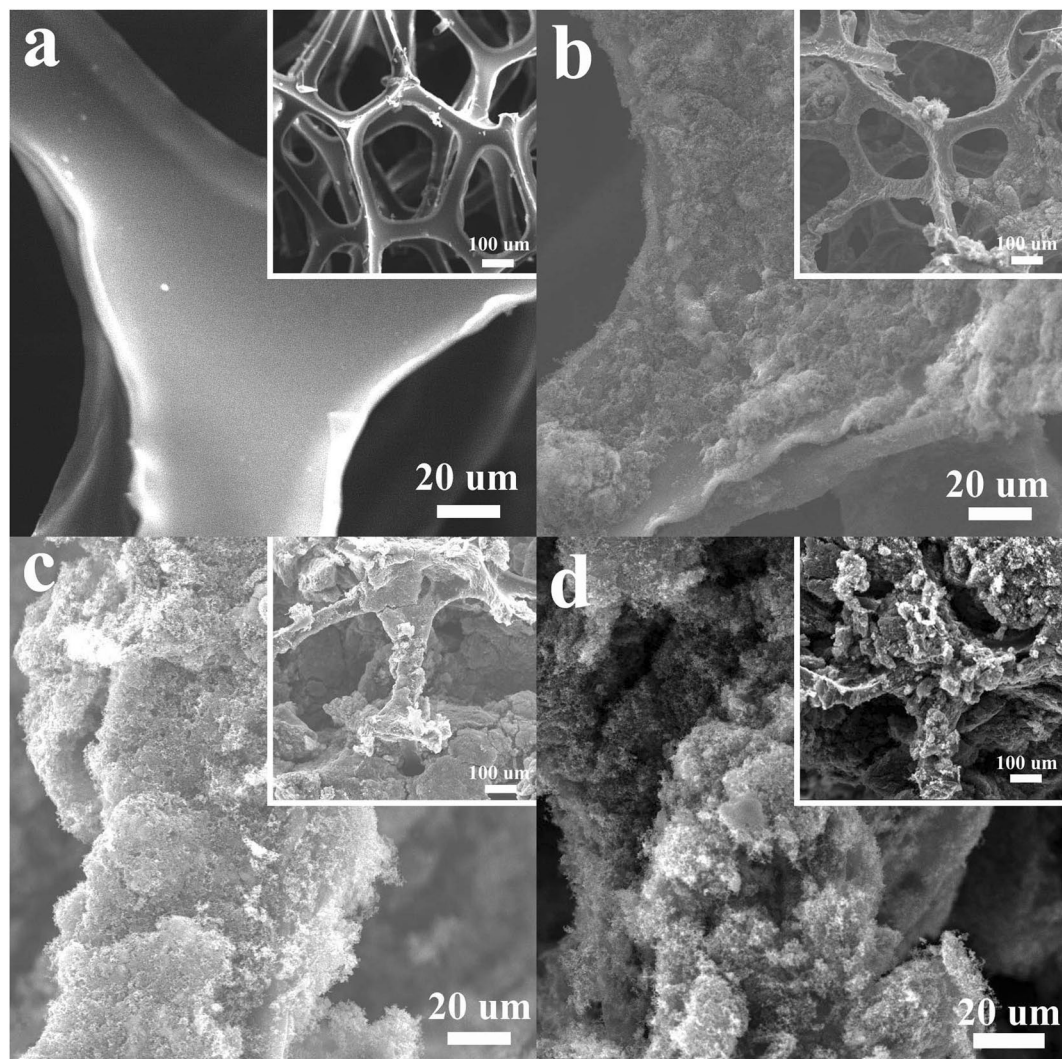
**Figure 2.** High resolution SEM images of (**a**) commercial sponge and floating air cathodes with different dipping-drying times, including (**b**) once, (**c**) three times and (**d**) six times. The insets are low resolution SEM images.

To evaluate the ORR performance of FACs with various dipping times, linear sweep voltammetry was measured. Due to the same catalytic component, the onset potentials of all FACs were −0.27 V vs. Ag/AgCl (Fig. S5). However, the ORR performance of FACs improved with dipping times. At −1.0 V vs. Ag/AgCl, only −4.6 mA of ORR current was produced on the DT1 FAC, much less than −18.1 mA for DT2. Raising dipping times resulted in increasing ORR current from −31.2 mA for DT3 to −42.5 mA for DT4 and −51.2 mA for DT5. When dipping time was eight, the ORR current reached a maximum of −63.2 mA, slightly larger than those for DT6 (−61.4 mA) and DT7 (−58.3 mA, Fig. S5). The improved ORR performance with DTs was attributed to higher active surface area and lower resistance that resulted from the increased catalyst mass loading. This was consistent with previous studies that mass loading of catalyst, ECSA and electrical conductivity of electrode were positively correlated with the performance of electrochemical systems[34,37]. Thus, when the same set voltage of 2 V was applied to produce H_2O_2, cathode potentials became more positive for the FACs with more DTs (Fig. S6). On average, the cathode potential on DT6 FAC was −0.63 V, a little more positive than −0.68 V on DT5 and −0.71 V on DT4. When dipping times were two or three, the average cathode potential was close, approximately −0.75 V (DT3) and −0.78 V (DT2). The FAC that was dipped only once had the most negative cathode potential of −0.88 V (Fig. S6), suggesting the worst cathode performance.

Produced H_2O_2 were measured using FACs with different dipping times. With the fixed set voltage of 2 V, the cathodic current and H_2O_2 production showed a positive relationship with the DTs of FACs from once to six times (Figs 3c and S7), attributing to the increasing mass loading, decreasing ohmic resistance and increasing ECSA. When the dipping times were six, the H_2O_2 concentration reached a maximum of 177.9 ± 26.1 mg L^{-1} at 90 min, slightly more than 158.7 ± 26.5 mg L^{-1} for five times (Fig. 3c). Lowering the DTs of FAC led to decreased H_2O_2 concentration from 122.2 ± 13.1 mg L^{-1} for four times to 65.6 ± 2.8 mg L^{-1} for twice (Fig. 3c). Only 17.2 ± 7.2 mg L^{-1} H_2O_2 generated if the sponge was dipped into CB/PTFE solution only once (Fig. 3c). The
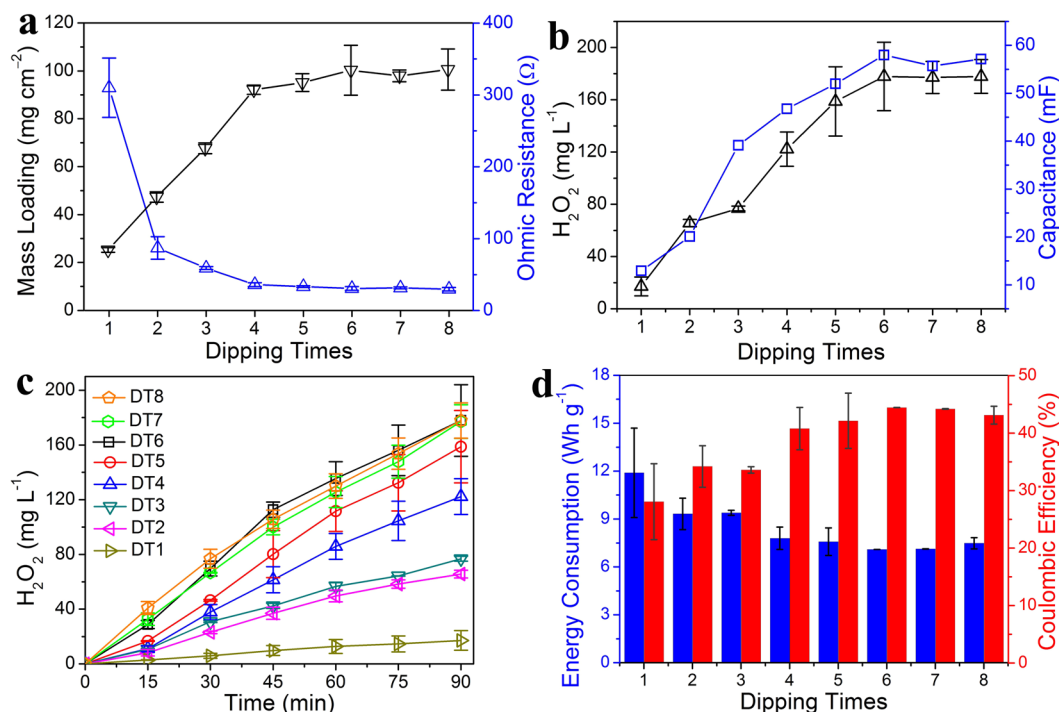
Figure 3. (**a**) Mass loading and ohmic resistances, (**b**) H_2O_2 production at 90 min and capacitance of electrochemical double layer, (**c**) H_2O_2 production with different reaction time, and (**d**) energy consumption and coulombic efficiency at 90 min of floating air cathodes with different dipping times.

improved H_2O_2 concentration with DTs from once to six times resulted from larger cathodic current (Fig. S7) and higher coulombic efficiency (Fig. 3d). However, after six times of dipping, the FACs showed similar electrochemical performance, leading to stable H_2O_2 generation of $177.1 \pm 12.2 \, mg \, L^{-1}$ for seven times and $177.8 \pm 12.9 \, mg \, L^{-1}$ for eight times (Fig. 3c).

Normalized energy consumption was evaluated for the H_2O_2 production using the FACs. The lowest consumed energy of $7.1 \pm 0.003 \, Wh \, g^{-1}$ was obtained at six dipping times for the FACs, close to $7.1 \pm 0.01 \, Wh \, g^{-1}$ at seven times, $7.5 \pm 0.35 \, Wh \, g^{-1}$ at eight times (Fig. 3d). With the decreased dipping times, energy consumption gradually increased from 7.6 ± 0.9 (five times) to 11.9 ± 2.8 (once) $Wh \, g^{-1}$ due to the increased ohmic resistance. The FAC was further evaluated by comparing its energy consumption with those of CB-based gas diffusion electrodes (GDEs) reported previously (Table 1)[13,22,27,38–41]. The energy consumption obtained here were lower than those with conventional CB-based GDEs (7.45–$22.1 \, Wh \, g^{-1}$, Table 1)[13,22,27,40]. For the modified cathodes with CoPc or FePc addition, the energy consumption was higher to be 30.8–$165 \, Wh \, g^{-1}$ [39,41]. The cathode with tert-butyl-anthraquinone (TBAQ) addition showed superior performance ($6.0 \, Wh \, g^{-1}$)[38] due to improved two-electron transfer selection, indicating that the energy consumption in our system could be further lowered with the improvement of catalyst activity.

Effect of applied voltages on H_2O_2 generation. H_2O_2 production was measured when applying different voltages using the FAC of DT6. With the set voltage increasing from $2.0 \, V$ to $5.0 \, V$, cathodic current gradually increased from $25.6 \, mA$ to $170.9 \, mA$ (Fig. S8), suggesting that oxygen reduction on the FAC dramatically enhanced. This huge ORR enhancement led to the improving performance of H_2O_2 generation via two-electron ORR pathway. As a result, the increase of H_2O_2 concentration with applied voltage was from $177.9 \pm 26.1 \, mg \, L^{-1}$ at $2.0 \, V$ to $488.6 \pm 77.5 \, mg \, L^{-1}$ at $3.0 \, V$ and $896.4 \pm 10.3 \, mg \, L^{-1}$ at $4.0 \, V$ (Fig. 4a). At the set voltage of $5.0 \, V$, the DT6 FAC produced a maximum of $1062.1 \pm 79.4 \, mg \, L^{-1}$ H_2O_2 within 90 min (Fig. 4a).

Normalized H_2O_2 generating rate was calculated to evaluate the performance of FAC-based electro-generation system. H_2O_2 generating rate showed a positive relationship with the applied voltage from $2.0 \, V$ to $5.0 \, V$ (Fig. 4b). At the fixed voltage of $2.0 \, V$, H_2O_2 was generated at the rate of only 0.46–$0.60 \, mg \, h^{-1} \, cm^{-2}$, far less than 1.30–$1.76 \, mg \, h^{-1} \, cm^{-2}$ at $3.0 \, V$ and 2.38–$3.46 \, mg \, h^{-1} \, cm^{-2}$ at $4.0 \, V$ (Fig. 4b). When $5.0 \, V$ of voltage was applied, the DT6 FAC produced H_2O_2 at a maximum rate of 2.82–$5.80 \, mg \, h^{-1} \, cm^{-2}$ (Fig. 4b). However, within 90 min of electrochemical treatment, H_2O_2 generating rate gradually decreased from $5.80 \pm 0.85 \, mg \, h^{-1} \, cm^{-2}$ at 15 min to $2.82 \pm 0.21 \, mg \, h^{-1} \, cm^{-2}$ at 90 min (Fig. 4b), attributing to enhanced H_2O_2 electro-decomposition (H_2O_2 reduction at cathode[1,18,42,43] and oxidation at anode[42,43]) from the rise of accumulated H_2O_2 concentration and electrode potential. The rate of $5.80 \pm 0.85 \, mg \, h^{-1} \, cm^{-2}$ to generate H_2O_2 obtained by FAC was higher than many reported GDEs (2.62–$4.41 \, mg \, h^{-1} \, cm^{-2}$, Table 1)[22,38,39,41]. In the electrochemical flow-by reactors, H_2O_2 generating rate could be improved to 15.53–$17.41 \, mg \, h^{-1} \, cm^{-2}$ (Table 1)[27,40] due to low solution resistance derived from the extremely small interelectrode gap (2.0–$6.5 \, mm$). In addition, concentrated alkaline solution as highly-conductive and high-pH electrolyte was beneficial for electro-reduction of oxygen, resulting in an ultrahigh H_2O_2 generating

Electrode	Electrode Orientation and Area	Catalyst	Volume and Type of Electrolyte	Electrochemical Method	H$_2$O$_2$ Concentration@Time	H$_2$O$_2$ Generating Rate (mg h^{-1} cm^{-2})	Energy Consumption (Wh g^{-1})	ref.
Floating Air Cathode	Horizon, 12.56 cm^2	Carbnon Black (CB)	50 mL, 100 mM Na$_2$SO$_4$	a fixed voltage of 2 V	177.9 ± 26.1 mg L^{-1}, 90 min	0.46–0.60	5.9–7.1	This work
Floating Air Cathode	Horizon, 12.56 cm^2	CB	50 mL, 100 mM Na$_2$SO$_4$	a fixed voltage of 5 V	1062.1 ± 79.4 mg L^{-1}, 90 min	2.82–5.80	11.1–23.8	This work
Gas Diffusion Cathode	Vertical, 20 cm^2	CB, tert-butyl-anthraquinone	400 mL, 100 mM K$_2$SO$_4$, 100 mM H$_2$SO$_4$	a fixed potential of −1.1 V vs. SCE	301 mg L^{-1}, 90 min	4.01	6.0	[38]
Gas Diffusion Cathode	Vertical, 100 cm^2	CB	1 L, 1 g L^{-1} Na$_2$SO$_4$ + H$_2$SO$_4$, pH = 3	a fixed current of 3 A	1000 mg L^{-1}, 35 min	17.14	7.45	[27]
Gas Diffusion Cathode	Vertical, 20 cm^2	CB	400 mL, 1000 mM KOH	a fixed potential of −1.1 V vs. Ag/AgCl	3370 mg L^{-1}, 90 min	44.93	8.0	[13]
Gas Diffusion Cathode	Vertical, 14.13 cm^2	CB	200 mL, 50 mM Na$_2$SO$_4$	a fixed current of 100 mA	556 mg L^{-1}, 180 min	2.62	8.6	[22]
Gas Diffusion Cathode	Vertical, 20 cm^2	CB	1.5 L, 100 mM K$_2$SO$_4$, 100 mM H$_2$SO$_4$	a fixed potential of −2.25 V vs. Ag/AgCl	414 mg L^{-1}, 120 min	15.53	22.1	[40]
Gas Diffusion Cathode	Vertical, 20 cm^2	CB, Cobalt (II) phthalocyanine	400 mL, 100 mM K$_2$SO$_4$, 100 mM H$_2$SO$_4$	a fixed potential of −0.7 V vs. Ag/AgCl	331 mg L^{-1}, 90 min	4.41	30.8	[39]
Gas Diffusion Cathode	Vertical, 20 cm^2	CB, Iron (II) phthalocyanine	400 mL, 100 mM K$_2$SO$_4$, 100 mM H$_2$SO$_4$	a fixed potential of −1.0 V vs. Ag/AgCl	240 mg L^{-1}, 90 min	3.2	165	[41]

Table 1. The comparisons of energy consumption of H$_2$O$_2$ production and H$_2$O$_2$ generating rate using the floating air cathode and other gas diffusion electrodes.
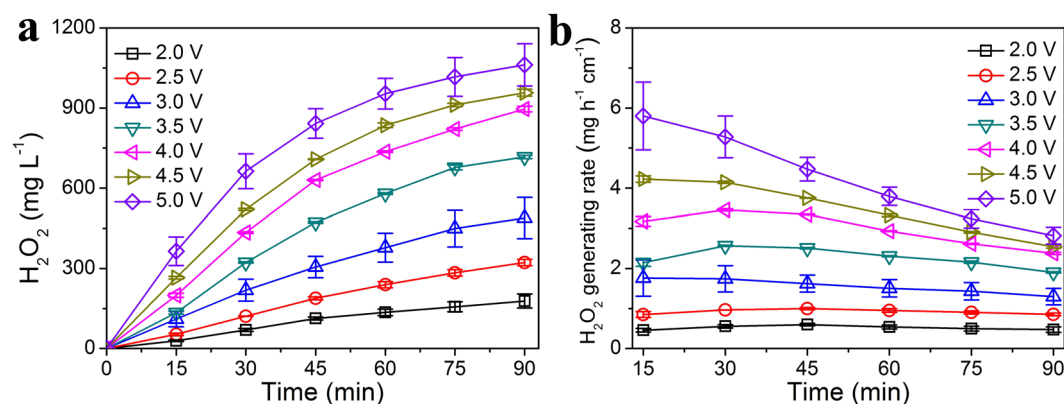

Figure 4. (**a**) H$_2$O$_2$ production and (**b**) H$_2$O$_2$ generating rate with different reaction time of floating air cathodes at different applied voltages.

rate of 44.93 mg h^{-1} cm^{-2} (Table 1)[13]. Therefore, H$_2$O$_2$ generating rate of FAC could be further improved by decreasing solution resistance and increasing electrolyte pH.

Effect of different O$_2$ supplies and electrode relative positions on the cathode performance.
To investigate the effect of different O$_2$ supplies on the cathode performance, H$_2$O$_2$ generation under four working modes was measured. These modes represented several different types of oxygen supply approach to the 3-D sponge-based electrode in the ORR system (Figs 5a and S1). The M1 working mode enabled continuous O$_2$ supply of the FAC from air and anodic OER, resulting in the H$_2$O$_2$ production of 177.9 ± 26.1 mg L^{-1} within 90 min (Fig. 5b). The generated H$_2$O$_2$ concentration decreased to 146.3 ± 26.3 mg L^{-1} for M2 (O$_2$ only from air) and 61.2 ± 1.4 mg L^{-1} for M3 (O$_2$ only from anodic OER, Fig. 5b). The appreciable decrease in H$_2$O$_2$ concentration could be contributed to the increase of resistances (insert of Fig. 5c) and reduced O$_2$ supply, indicating the significance of dual O$_2$ supply for the energy-efficient H$_2$O$_2$ production using the FAC. Under the M4 condition with the submerged cathode and misplaced anode, the H$_2$O$_2$ generation of 34.1 ± 1.6 mg L^{-1} at 90 min (Fig. 5b) might be attributed to the little oxygen adsorbed in the sponge-based electrode and dissolved in the electrolyte (dissolved oxygen of 7.8–15.7 mg L^{-1}, Fig. S9). Due to the lack of continuous oxygen supply, the cathodic current gradually decreased from 40 mA to 2 mA in the initial 45 min (Fig. 5c).

Compared with submerged cathodes (M3 and M4), the cathodic currents of FACs (M1 and M2) with O$_2$ supply from air were relatively stable during the whole 90-min operation (Fig. 5c), indicating the steady O$_2$ diffusion
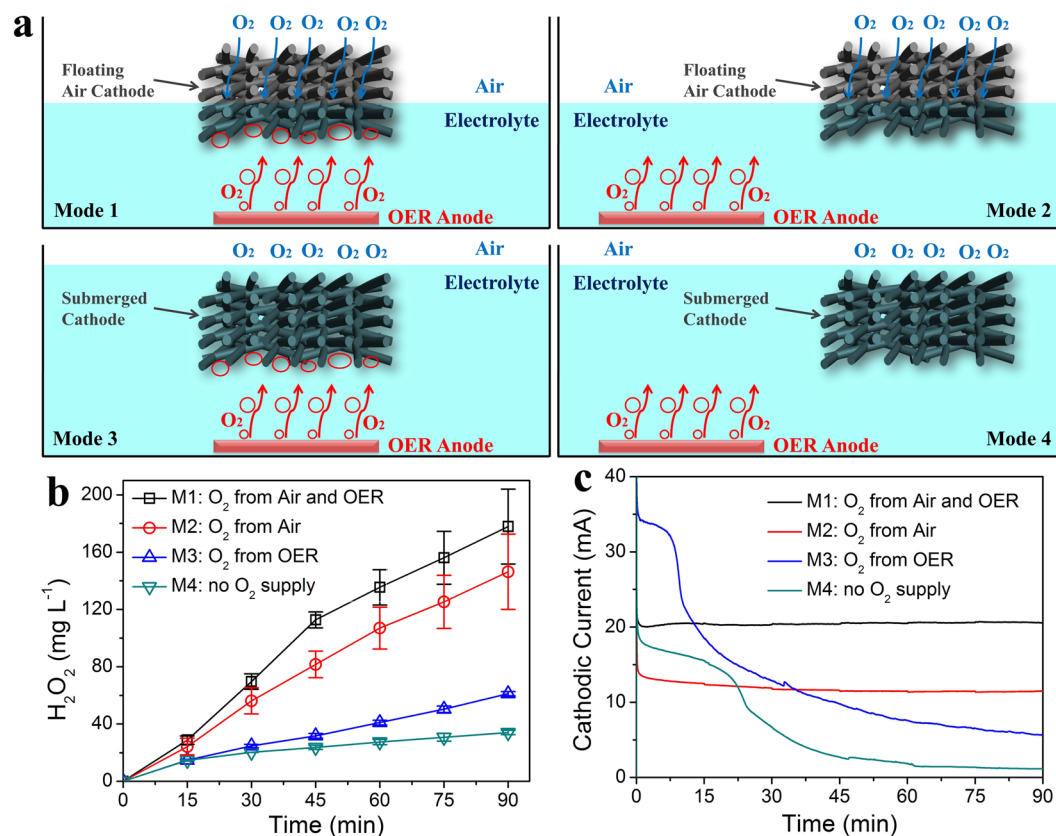
Figure 5. (**a**) Schematic illustrations of four working modes; (**b**) H_2O_2 production and (**c**) ORR cathodic current of the sponge-based electrodes under four working models with the set voltage of 2 V.

paths in FACs. The stable current production with FACs (M1 of 20.57 mA and M2 of 11.49 mA) were higher than those with submerged cathodes (M3 of 5.64 mA and M4 of 1.15 mA, Fig. 5c). The higher cathodic current with FACs resulted from passive O_2 diffusion from air through the three-phase interface. When cathodes were submerged, the O_2 transfer was greatly hindered in aqueous solution. Therefore, the H_2O_2 generation from FACs was also much better than that from submerged cathodes.

For the FACs (M1 and M2) and submerged cathodes (M3 and M4), the relative position between cathode and anode also affected their electrochemical performance. From a comparison of either M1&M2 or M3&M4, the cathodic current with a facing position was larger than those with a misplaced position (M1 of 20.6 mA > M2 of 11.5 mA and M3 of 5.6 mA > M4 of 1.2 mA, Fig. 5c). The decreased cathodic current with a misplaced position could be attributed to the increased solution resistance, electric field lines change and less oxygen supply without the utilization of OER produced oxygen. When the sponge-based cathodes were misplaced with MMO anodes, the solution resistance increased from 14.7 Ω for M1 to 27.7 Ω for M2 and from 7.4 Ω for M3 to 16.2 Ω for M4 (Fig. S10). Therefore, consistent with the trend of cathodic current, the H_2O_2 production with a facing position was much higher than that with a misplaced position (Fig. 5b).

Coulombic efficiency was evaluated for the sponge electrodes under all four working modes. The CEs for FACs ranged from 39.7 ± 0.2% to 77.7 ± 4.4%, and the highest value of 77.7 ± 4.4% was obtained for M2 at 30 min (Fig. S11). However, for submerged cathodes, the CEs were lower than 30%, and the lowest CE of 15.9 ± 1.1% for M3 at 15 min resulted from the largest cathodic current and least H_2O_2 generation (Fig. S11). In general, the CEs for FACs (39.7 ± 0.2%–77.7 ± 4.4%) were also much higher than that for submerged cathodes (15.9 ± 1.1%–30.8 ± 2.7%, Fig. S11).

Stability of the FAC for H_2O_2 production. To evaluate the working stability of FAC with dual O_2 supplies, the H_2O_2 generation with a fixed voltage of 2 V (the actual cathode potential ranged between −0.68 V and −0.56 V, Fig. S6) in a batch of experiments by changing the electrolyte every 90 min was investigated. Under the M1 working mode, the varying range of cathodic current on the FAC was moderate (18–24 mA, Fig. 6a), indicating the relatively stable performance of the FAC. In each run, the linear increase of H_2O_2 production also reflected the stability and sustainability of two-electron ORR process (Fig. 6b). The yield of H_2O_2 was almost stable with a fluctuation during ten cycles, and the fluctuating range of H_2O_2 concentration was from 187 to 237 mg L^{-1} (Fig. 6b). The fluctuation of H_2O_2 production could be partially resulted from the variation of ECSA of FAC in different cycles as the cathode floated freely on the solution/air interface. This result showed that the electrochemical ORR system using the FAC was capable of working stably, representing a promising system for energy efficient H_2O_2 production.
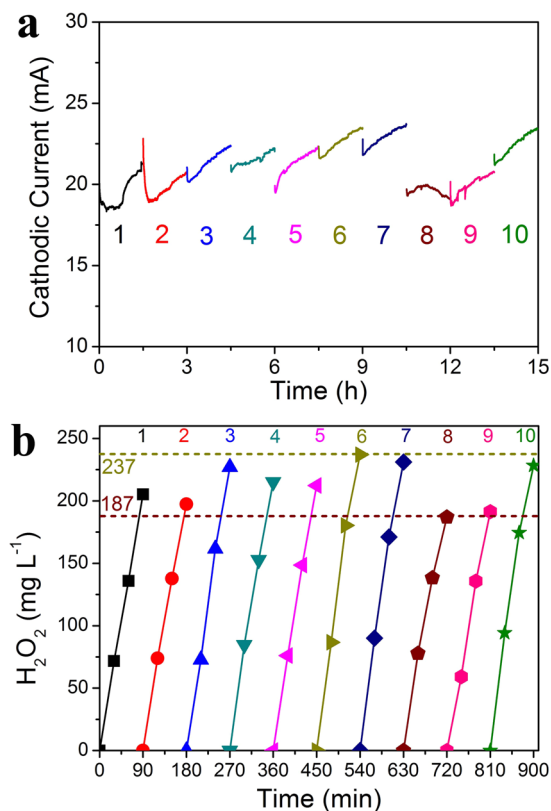
Figure 6. (**a**) ORR cathodic current and (**b**) H_2O_2 generation of ten cycles by changing the electrolyte every 90 min.

Conclusions

In this study, the floating air cathodes were fabricated using commercially available sponge with a simple dipping-drying method. When the cathode floated on top of the OER anode, it had dual oxygen supply sources both from the air and anodic OER. The optimized FAC produced a maximum H_2O_2 production of $177.9 \pm 26.1\,mg\,L^{-1}$ within 90 min, and had a low energy consumption of $7.1 \pm 0.003\,Wh\,g^{-1}$ and good working stability. The features make the FAC a promising option to *in situ* H_2O_2 production in scale up applications for either environmental remediation or industrial applications.

References

1. Brillas, E., Sirés, I. & Oturan, M. A. Electro-Fenton process and related electrochemical technologies based on Fenton's reaction chemistry. *Chem. Rev.* **109**, 6570–6631 (2009).
2. Cheng, M. *et al.* Hydroxyl radicals based advanced oxidation processes (AOPs) for remediation of soils contaminated with organic compounds: A review. *Chem. Eng. J.* **284**, 582–598 (2016).
3. Frangos, P. *et al.* Improvement of the degradation of pesticide deethylatrazine by combining UV photolysis with electrochemical generation of hydrogen peroxide. *Chem. Eng. J.* **291**, 215–224 (2016).
4. Yuan, D. *et al.* Solar Thermo-coupled Electrochemical Oxidation of Aniline in Wastewater for the Complete Mineralization Beyond an Anodic Passivation Film. *Sci. Rep.* **8**, 3103 (2018).
5. Campos-Martin, J. M., Blanco-Brieva, G. & Fierro, J. L. Hydrogen peroxide synthesis: an outlook beyond the anthraquinone process. *Angew. Chem. Int. Ed.* **45**, 6962–6984 (2006).
6. Moreira, F. C., Boaventura, R. A. R., Brillas, E. & Vilar, V. J. P. Electrochemical advanced oxidation processes: A review on their application to synthetic and real wastewaters. *Appl. Catal. B-Environ.* **202**, 217–261 (2017).
7. Tang, P. *et al.* Highly dispersed Pd catalyst for anthraquinone hydrogenation supported on alumina derived from a pseudoboehmite precursor. *Appl. Catal. A-Gen.* **469**, 312–319 (2014).
8. Guo, Y., Dai, C., Lei, Z., Chen, B. & Fang, X. Synthesis of hydrogen peroxide over Pd/SiO2/COR monolith catalysts by anthraquinone method. *Catal. Today* **276**, 36–45 (2016).
9. Barazesh, J. M., Hennebel, T., Jasper, J. T. & Sedlak, D. L. Modular advanced oxidation process enabled by cathodic hydrogen peroxide production. *Environ. Sci. Technol.* **49**, 7391–7399 (2015).
10. Zhang, H., Wan, X., Li, G. & Zhang, F. A Three-electrode Electro-Fenton System Supplied by Self-generated Oxygen with Automatic pH-regulation for Groundwater Remediation. *Electrochim. Acta* **250**, 42–48 (2017).
11. Yuan, S., Fan, Y., Zhang, Y., Tong, M. & Liao, P. Pd-catalytic *in situ* generation of H_2O_2 from H_2 and O_2 produced by water electrolysis for the efficient electro-fenton degradation of rhodamine B. *Environ. Sci. Technol.* **45**, 8514–8520 (2011).
12. Siahrostami, S. *et al.* Enabling direct H_2O_2 production through rational electrocatalyst design. *Nat. Mater.* **12**, 1137–1143 (2013).
13. Barros, W. R. P., Ereno, T., Tavares, A. C. & Lanza, M. R. V. *In Situ* Electrochemical Generation of Hydrogen Peroxide in Alkaline Aqueous Solution by using an Unmodified Gas Diffusion Electrode. *ChemElectroChem* **2**, 714–719 (2015).
14. Truesdale, G. & Downing, A. Solubility of oxygen in water. *Nature* **173**, 1236–1236 (1954).
15. Truesdale, G., Downing, A. & Lowden, G. The solubility of oxygen in pure water and sea - water. *J. Chem. Technol. Biotechnol.* **5**, 53–62 (1955).

16. Kallikragas, D. T., Plugatyr, A. Y. & Svishchev, I. M. High Temperature Diffusion Coefficients for O_2, H_2, and OH in Water, and for PureWater. *J. Chem. Eng. Dat.* **59**, 1964–1969 (2014).
17. Han, P. & Bartels, D. M. Temperature dependence of oxygen diffusion in H_2O and D_2O. *J. Physic. Chem.* **100**, 5597–5602 (1996).
18. Qiang, Z., Chang, J.-H. & Huang, C.-P. Electrochemical generation of hydrogen peroxide from dissolved oxygen in acidic solutions. *Water Res.* **36**, 85–94 (2002).
19. Liu, H. *et al.* A novel electro-Fenton process for water treatment: reaction-controlled pH adjustment and performance assessment. *Environ. Sci. Technol.* **41**, 2937–2942 (2007).
20. Carnes, B. & Djilali, N. Systematic parameter estimation for PEM fuel cell models. *J. Pow. Sour.* **144**, 83–93 (2005).
21. Zhang, F., Chen, G., Hickner, M. A. & Logan, B. E. Novel anti-flooding poly(dimethylsiloxane) (PDMS) catalyst binder for microbial fuel cell cathodes. *J. Pow. Sour.* **218**, 100–105 (2012).
22. Yu, X., Zhou, M., Ren, G. & Ma, L. A novel dual gas diffusion electrodes system for efficient hydrogen peroxide generation used in electro-Fenton. *Chem. Eng. J.* **263**, 92–100 (2015).
23. Lu, Y., Liu, G., Luo, H. & Zhang, R. Efficient *in-situ* production of hydrogen peroxide using a novel stacked electrosynthesis reactor. *Electrochim. Acta* **248**, 29–36 (2017).
24. Abdullah, G. H. & Xing, Y. Hydrogen Peroxide Generation in Divided-Cell Trickle Bed Electrochemical Reactor. *Ind. Eng. Chem. Res.* **56**, 11058–11064 (2017).
25. Ahn, Y., Zhang, F. & Logan, B. E. Air humidity and water pressure effects on the performance of air-cathode microbial fuel cell cathodes. *J. Pow. Sour.* **247**, 655–659 (2014).
26. Li, H. *et al.* A review of water flooding issues in the proton exchange membrane fuel cell. *J. Pow. Sour.* **178**, 103–117 (2008).
27. Agladze, G. R., Tsurtsumia, G. S., Jung, B. I., Kim, J. S. & Gorelishvili, G. Comparative study of hydrogen peroxide electro-generation on gas-diffusion electrodes in undivided and membrane cells. *J. Appl. Electrochem.* **37**, 375–383 (2007).
28. Oturan, M. A., Oturan, N., Lahitte, C. & Trevin, S. Production of hydroxyl radicals by electrochemically assisted Fenton's reagent: Application to the mineralization of an organic micropollutant, pentachlorophenol. *J. Electroanal. Chem.* **507**, 96–102 (2001).
29. Yuan, S., Gou, N., Alshawabkeh, A. N. & Gu, A. Z. Efficient degradation of contaminants of emerging concerns by a new electro-Fenton process with Ti/MMO cathode. *Chemosphere* **93**, 2796–2804 (2013).
30. Qian, A., Yuan, S., Zhang, P. & Tong, M. A New Mechanism in Electrochemical Process for Arsenic Oxidation: Production of H_2O_2 from Anodic O_2 Reduction on the Cathode under Automatically Developed Alkaline Conditions. *Environ. Sci. Technol.* **49**, 5689–5696 (2015).
31. Xie, X. *et al.* Carbon nanotube-coated macroporous sponge for microbial fuel cell electrodes. *Energy Environ. Sci.* **5**, 5265–5270 (2012).
32. Zhang, H. *et al.* Highly Crystallized Cubic Cattierite CoS_2 for Electrochemically Hydrogen Evolution over Wide pH Range from 0 to 14. *Electrochim. Acta* **148**, 170–174 (2014).
33. Li, Y. *et al.* Amorphous Co–Mo–S ultrathin films with low-temperature sulfurization as high-performance electrocatalysts for the hydrogen evolution reaction. *J. Mater. Chem. A* **4**, 13731–13735 (2016).
34. Jiang, J., Li, G., Li, Z., Zhang, X. & Zhang, F. An Fe–Mn binary oxide (FMBO) modified electrode for effective electrochemical advanced oxidation at neutral pH. *Electrochim. Acta* **194**, 104–109 (2016).
35. Zhang, H. *et al.* A metallic CoS_2 nanopyramid array grown on 3D carbon fiber paper as an excellent electrocatalyst for hydrogen evolution. *J. Mater. Chem. A* **3**, 6306–6310 (2015).
36. Zhang, H. *et al.* Amorphous Co-doped MoS_2 nanosheet coated metallic CoS_2 nanocubes as an excellent electrocatalyst for hydrogen evolution. *J. Mater. Chem. A* **3**, 15020–15023 (2015).
37. Zhang, X., Xia, X., Ivanov, I., Huang, X. & Logan, B. E. Enhanced activated carbon cathode performance for microbial fuel cell by blending carbon black. *Environ. Sci. Technol.* **48**, 2075–2081 (2014).
38. Valim, R. B. *et al.* Electrogeneration of hydrogen peroxide in gas diffusion electrodes modified with tert-butyl-anthraquinone on carbon black support. *Carbon* **61**, 236–244 (2013).
39. Barros, W. R. P., Reis, R. M., Rocha, R. S. & Lanza, M. R. V. Electrogeneration of hydrogen peroxide in acidic medium using gas diffusion electrodes modified with cobalt (II) phthalocyanine. *Electrochim. Acta* **104**, 12–18 (2013).
40. Reis, R. M. *et al.* Use of Gas Diffusion Electrode for the *In Situ* Generation of Hydrogen Peroxide in an Electrochemical Flow-By Reactor. *Ind. Eng. Chem. Res.* **51**, 649–654 (2012).
41. Silva, F. L., Reis, R. M., Barros, W. R. P., Rocha, R. S. & Lanza, M. R. V. Electrogeneration of hydrogen peroxide in gas diffusion electrodes: Application of iron (II) phthalocyanine as a modifier of carbon black. *J. Electroanal. Chem.* **722**, 32–37 (2014).
42. Brillas, E., Bastida, R. M., Llosa, E. & Casado J. Electrochemical Destruction of Aniline and 4-Chloroaniline for Wastewater Treatment Using a Carbon-PTFE O_2-Fed Cathode. *J. Electrochem. Soc.* **142**, 1733–1741 (1995).
43. Zhou, W. *et al.* Drastic enhancement of H_2O_2 electro-generation by pulsed current for ibuprofen degradation: Strategy based on decoupling study on H_2O_2 decomposition pathways. *Chem. Eng. J.* **338**, 709–718 (2018).

Acknowledgements

Author Contributions

Haichuan Zhang conceived and conducted the experiments and wrote the manuscript. Yingjie Li analysed the results and reviewed the manuscript. Hao Zhang conducted the SEM characterizations. Guanghe Li reviewed the manuscript. Fang Zhang conceived the experiments and reviewed the manuscript.

Additional Information

Supplementary information accompanies this paper at https://doi.org/10.1038/s41598-018-37919-3.

Competing Interests: The authors declare no competing interests.

Publisher's note: Springer Nature remains neutral with regard to jurisdictional claims in published maps and institutional affiliations.